Minimal requirements for membrane adaptation of the bacterial model organism *M. extorquens*

Grzegorz Chwastek [1], Michał A. Surma[2,] ORCID, Sandra Rizk[1,] ORCID, Daniel Grosser[3], Oksana Lavrynenko[4], Andrej Schevchenko[4], Magdalena Rucińska [1] ,Helena Jambor[5,]ORCID, James Sáenz[1,*,]ORCID

1 Technische Universität Dresden, B CUBE, Tatzberg 41, Dresden, DE

2 Łukasiewicz Research Network – PORT Polish Center for Technology Development, Stabłowicka 147, Wrocław, PL

3 DZD-Paul Langerhans Institute Dresden, Fetscherstraße 74, Dresden, DE

4 Max Planck Institute of Molecular Cell Biology and Genetics, Pfotenhauerstrasse 108, Dresden, DE

5 Technische Universität Dresden, Medizinische Fakultät, Fetscherstraße 74, Dresden, DE

* corresponding author and lead contact: james.saenz@tu-dresden.de

Keywords Lipidomics, Membrane organization, Adaptation, Lipidome adaption resource

Abstract

Cells, from microbes to man, adapt their membranes in response to the environment to maintain functionality. How cells sense environmental change/stimuli and adapt their membrane accordingly is unclear. In particular, how lipid composition changes and what lipid structural features are necessary for homeostatic adaptation remains relatively undefined. Here, we examine the simple yet adaptive lipidome of the plant-associated Gram-negative bacterium *Methylobacterium extorquens* over a range of chemical and physical conditions. Using shotgun lipidomics, we explored adaptivity over varying temperature, hyperosmotic and detergent stress, carbon sources, and cell density. Globally, we observed that as few as 10 lipids, representing ca. 30% of the lipidome, characterized by 9 structural features account for 90% of the total changes. We revealed that variations in lipid structural features are not monotonic over a given range of conditions (e.g. temperature) and are not evenly distributed across lipid classes. Thus, despite the compositional simplicity of this lipidome, the patterns in lipidomic remodeling suggest a highly adaptive mechanism with many degrees of freedom. Our observations reveal constraints on the minimal lipidomic requirements for an adaptive membrane and provide a resource for unraveling the design principles of living membranes.

1. Introduction

All organisms have at least one membrane that is crucial for compartmentalizing and coordinating biochemical processes within the cell. And yet, nearly a century since the discovery that membranes are made of a lipid bilayer (Gorter and Grendel, 1925) and half a century since integral membrane proteins were proposed in the Fluid Mosaic model (Singer and Nicolson, 1972) we still lack fundamental insight into the design principles required to engineer a functional cell membrane. Much of the membrane's functionality is associated with the activity of membrane proteins, which perform a diverse range of tasks from signaling to transport. The activity of such proteins is in turn crucially dependent on the biophysical properties of the membrane such as viscosity, thickness, curvature and bilayer asymmetry (Hunte and Richers, 2008; Klose et al., 2013; Pomorski and Menon, 2006; Sanders and Mittendorf, 2011). These properties are largely dictated by membrane lipids (Ernst et al., 2016; van Meer et al., 2008).

Cells produce many lipids with different structures that, in their unique combinations, determine the membrane's biophysical state. Moreover, cellular lipidomes can vary from tens, for example in the bacterial lipidome reported here, to hundreds of individual lipid species in mammalian cells (van Meer et al., 2008). A major challenge in membrane research is therefore to understand how cells regulate individual lipid abundances to maintain an adaptive, functional membrane. Recent progress reconstituting synthetic membranes from the bottom up is paving the way towards the goal of building a self-sustaining adaptive membrane and presently one of the challenges is to implement adaptive lipid remodeling (Hardy et al., 2015). Complex lipidomes can be remodeled to modulate collective membrane properties such as viscosity, lipid packing, thickness and phase properties (Klose et al., 2013). For instance, increasing the proportion of lipids containing double bonds (acyl chain saturation) or changing the number or position of double bonds along the phospholipid acyl chains, can alter the overall membrane viscosity (Quinn, 1981).

Singular observations of lipidome composition however do not inform which properties the cell membrane senses and adapts to, nor which minimal suite of lipid structure are required for swift adaptation. Lipidomics has provided global insights into the complexity of cellular lipidomes from yeast to man and can provide insight into how cells remodel lipid composition during adaptation. To date however there still are only few studies systematically characterizing lipidomic remodeling across a range of conditions and stressors. The most comprehensive study of this kind was performed on yeast (Klose et al., 2012), whose lipidome contains over 150 unique lipids, providing unprecedented insight into the adaptation of a complex eukaryotic lipidome.

Complex organisms possess membranes with diverse and niche-specific functional requirements. While, understanding complex lipidomes is important, such systems are not ideal for exploring the fundamental principles underlying lipidome adaptation. Since all membranes require means to homeostatically adapt to perturbations (Kaiser et al., 2011), a simpler organism that is capable of adapting to a broad range of environmental conditions would be a more suitable model system to elucidate the minimal lipidomic requirements for adaptation. Bacteria are an attractive target for this endeavor since some are among the simplest organisms, capable of surviving over a broad range of environments, and many species have been well-characterized and established as model organisms for cell biology. Here, we characterized the lipidomic adaptivity of the Gram-negative bacterium *Methylobacterium extorquens*. *M. extorquens* has a small lipidome, with 25 phospholipid species as compared with over 100 in E. Coli (Jeucken et al., 2019). Despite its relatively small lipidome, as a plant- and soil-associated bacterium, *M. extorquens* must adapt to a broad range of chemical and physical conditions (Vorholt, 2012). We explored the lipidome variation over varying temperature, osmotic and detergent stress, carbon source, and cell density. Surprisingly, we find that most lipidome features remain stable, with only minimal modulations even under significant perturbations. However, other lipidome features are highly plastic and contribute to membrane adaptation. Analysis of structural features such as saturation, acyl-chain length or head-group revealed signatures of adaptive lipidomes. Globally, we observed that as few as 10 lipids, < 30% of all available species, account for the majority of lipidomic adaptation across all perturbations. The patterns of lipidome remodeling that we report here provide a resource for exploring the minimal design principles of living membranes and for designing an adaptive synthetic membrane.

2. Results and Discussion

2.1 Experimental Design

To determine lipidomic remodeling induced by environmental perturbations, we measured the lipidomes of *M. extorquens* under physical and chemical challenges to cellular membrane homeostasis (Figure 1a; Figure 1-Figure supplement 1a). To this end, we varied temperature, osmotic conditions, detergent stresses, carbon sources, and cell densities (Figure 1-Figure supplement 2a). Cells were harvested during early exponential growth to minimize their impact on media chemical composition. Temperature was varied from 6 to 30 ˚C to challenge the viscosity of the membranes. Salt (NaCl) and detergent (Triton X-100) concentration were varied to produce osmotic and detergent stresses, respectively. Cells were grown on two concentrations of methanol (0.1 and 1% v/v) as the

sole carbon source to evaluate the effect of metabolism on lipidomic remodeling. Finally, to characterize lipidomic adaptation at varying cell densities, cells were harvested at early, mid and late exponential, as well as stationary growth stages (Figure 1b). Cellular lipid content was analyzed by high resolution shotgun mass spectrometry (Ejsing et al., 2009) to determine absolute abundances of 25 phospholipids and two hopanoid species, distributed between 5 lipid classes and representing over 90 mol% of the lipidome of *M. extorquens* (Sáenz et al., 2015)(Figure 2).

It has been previously shown that *M. extorquens* produces lipids with 16 and 18 carbon atoms-long acyl chains, and with up to 2 double bonds per acyl chain (Bradley et al., 2017; Wallace et al., 1990). Consistently, the major PG, PE, and PC species have cumulative chain length of 36 or 34 carbons with two double bonds per lipid (e.g. 18:1/18:1 and 18:1/16:1) and minor species with up to 4 double bonds per lipid. We also observed methylation of diplopterol (2Me-DIP) which has previously been reported in cyanobacteria and methylotrophic bacteria including *Methylobacterium* (Bradley et al., 2017; Rashby et al., 2007; Stampf et al., 1991; Summons et al., 1999). Recent work suggests that 2-methylation may be particularly prevalent among plant-associated bacteria (Ricci et al., 2014). In the following sections, we dissect the data in Figure 2 in order to reveal patterns in lipidomic variation across experimental conditions.

2.2 **Lipidomic variation across experimental conditions**

To broadly characterize the effect of environmental perturbations on membrane remodeling, we evaluated the cumulative lipid variability for each growth condition. Presently there is no gold standard for evaluating lipidomic variability. Lipid variability has previously been reported as the variance over mean of lipid abundance (Klose et al., 2012). This analysis reveals how much a lipid varies relative to its abundance, such that even a very low abundance lipid that has a small change in relation to a total lipidome could have a high variance over mean. However, in this study we aimed to characterize variations that would have an impact on the bulk adaptive properties of the membrane. Since small changes in abundance do not have a considerable effect on the bulk adaptive properties of the membrane, we focused on lipids with high absolute changes in abundance. Therefore, we calculated lipid variability as the standard deviation of abundances over a range of conditions. The total lipidomic variability was then calculated as the aggregate standard deviation of relative abundance for all individual lipid species over the range of the various conditions (e.g. temperature, growth stage, etc.). (Figure 3a). This analysis revealed that temperature has by far the largest effect on lipidomic remodeling, with >2-fold more variability than any other condition. Surprisingly, the smallest effects were observed with detergent challenge.

To compare general lipidomic features for each individual experimental condition, we performed a principle component analysis (PCA) on lipid species abundances (Figure 3b). PCA is a method that allows for the comparison of multidimensional data by reducing variations down to two-dimensions called principle components. Distance between each point on the PCA plot is proportional to variation in lipid composition between conditions. Most conditions clustered closely with the standard growth condition, shown in red. Thus, lipid composition was not strongly affected by detergent, methanol, low salt concentrations, or during the progression through early, mid, and late growth stage. In stark contrast, bacteria grown at low temperatures, in stationary growth phase, or at high salt conditions (0.2 M NaCl) did not cluster with the standard growth condition, indicating a high extent of lipidome remodeling. Furthermore, temperature had an orthogonal effect compared to stationary growth and high salt conditions, indicating that a different set of lipidomic features is involved in responses to those conditions.

It is surprising that a membrane destabilizing detergent (Helenius, 1975) did not result in lipidomic remodeling. This could possibly be attributed to the ability of Gram-negative bacteria to resist chemicals through the robustness imparted by barrier function of lipopolysaccharide at the cell surface and active removal of toxins by multidrug transporters (Nikaido, 1996; 2003; Nikaido and Vaara, 1985; Piddock, 2006). The insensitivity of the lipidome to methanol was also unexpected. Klose et al (2012) showed that the yeast lipidome varied greatly with differing carbon substrates based on a similar PCA analysis. Our result suggests that methanol and succinate metabolism do not require different membrane properties in *M. extorquens*. Nonetheless, the dominant effect of temperature is consistent with the large diurnal temperature variations that *M. extorquens* must adjust to in its native habitat on plant leaf surfaces and in soils. It is possible that the mechanisms of lipidome adaptation and the lipidomic composition in *M. extorquens* have evolved to be particularly well-suited for temperature changes.

2.3 **Variation in individual lipid species**

We next examined the individual lipid species involved in membrane adaptation in *M. extorquens*. The highest abundance species generally show the largest degree of variability (Figure 4a and 4b). However, there are some low abundance species that exhibit large variations, notably lipids with 3 and 4 double bonds. An important point of emphasis is that low abundance or undetectable species at standard growth conditions can become major components under certain conditions, playing a crucial role in adaptation. The most striking result is that the majority of lipid species do not vary

substantially under any conditions, suggesting that only a small fraction of the lipidome is required for adaptive membranes.

We then asked how many and which lipid species are highly variable for each set of conditions. We defined the highly variable lipid species as those that account for 90% of the total lipidomic variability within any given condition. By this measure we observed that 10-13 lipids are highly variable over any given condition (Figure 4c), meaning that only around 30% of the lipidome is involved in remodeling during adaptation. Of these 10-13 highly variable lipids, 8 are highly variable over all of the conditions tested. These results revealed that only a fraction of the lipidome is involved in adaptive remodeling and point towards the minimum complexity of lipid species required for membrane adaptation. In principle, it is possible that as few as 8 lipid species could support adaptation over the range of experimental conditions examined in this study.

2.4 **Variation of lipid structural features**

Membrane biophysical properties are modulated by changes in the abundance of lipid structural features. For instance, increasing the number of double bonds per lipid reduces membrane viscosity during adaptation to decreasing temperature, whereas various lipid headgroups can impart curvature or surface charge. We analyzed how the various structural features of *M. extorquens* lipids are modulated to glean insight into their sense and response mechanisms of membrane adaptation.

Headgroup features were differently regulated, as PC, PE and PG were relatively plastic, whereas CL and diplopterols are relatively invariant (Figure 5a). For acyl chains, most of the variability is observed for lipids with 2 and 3 double bonds and with total chain length of 34-36 carbons (Figure 5b). When we group acyl chain features separately for each headgroup (e.g. PC-specific unsaturation) PC shows the largest variability for both unsaturation and chain length, whereas PG acyl chain features are nearly invariant. This shows that acyl chain features are regulated independently within each headgroup, and provides a starting recipe for designing a responsive synthetic lipidome.

To assess how much different features varied for each experimental condition we calculated the variance of lipid features for each range of conditions as depicted by the heat map in Figure 5c. The highest variation in lipid classes is observed over temperature and growth stage. Interestingly, total lipid unsaturation varies over temperature but is relatively invariant over all other conditions. The most variation in total lipid chain length varies with temperature and salt concentration. These results reveal that membrane adaptation of total lipid features exhibit different patterns in response to

different experimental conditions. This shows that the lipidomic adaptation mechanism is capable of unique, orthogonal responses to different perturbations.

2.5 **Progressive remodeling of lipids across experimental conditions**

Assessing lipidomic data for each step within each condition allows us to compare lipids as we go stepwise through the changes. For instance, how does the lipidome compare when the growth temperature is lowered from 30 to 20 to 13 and to 4 degrees, or as cells progress from early to mid, to late and finally to stationary growth phase? We again consider lipids grouped by their features as this allowed us to monitor structural variations that directly impact the membrane's biophysical properties (Figure 6; Figure 6-Figure supplement 1-4).

Class

Lipid class abundances are relatively invariant over most conditions (Figure 6). PC abundance increases with decreasing temperature, with a pronounced change at 6 ˚C. PE abundance increases considerably when cells are in stationary growth stage. These results suggest that lipid class distribution is only adjusted under extreme conditions.

Double Bonds

The total number of double bonds per lipid varies substantially with temperature and is nearly invariant for other conditions. As temperature decreases the abundances of DB3 and DB4 lipids increase, while abundances of DB1 and DB2 decrease. This contrasts with other organisms such as yeast where primarily DB1 and DB2 are adjusted with temperature change (Klose et al., 2012). It is possible that having additional double bonds enhances Methylobacterium's ability to adapt to broad temperatures that they experience on plant surfaces and in soils.

The variation of double bonds per lipid within each headgroup class is not evenly distributed across classes. For instance, for varying temperatures PC shows the highest remodeling whereas PG is nearly invariant. Additionally, for varying salt and growth stages where total unsaturation has little or negligible variability, class-specific PC-DB and CL-DB vary considerably. These variations in PC-DB and CL-DB are nearly equal and opposite resulting in no apparent change in total DB content.

Chain length

Total chain length is highly conserved across all conditions, and only varies substantially at 6 ˚C. Since total chain length has a large effect on membrane thickness, which in turn must be matched

with membrane protein transmembrane domain length, it is not surprising that this feature is so invariant. The large change in total CL at extreme low temperature suggests that the membrane must take extreme measures to adapt as it approaches the end of the range of viable growth temperature.

Similar to unsaturation, chain length within each headgroup class shows much higher variability than total chain length. For instance, from 30 to 20 ˚C total chain length remains constant while PC chain length decreases and is compensated for by increased chain length in PG, PE and CL. Similar remodeling is also observed for growth stage and salt concentration. Additionally, PC exhibits the highest chain length variation.

Diplopterol 2-methylation

A particularly striking variation was observed for the sterol analogue diplopterol and its 2-methylated derivative (Figure 7). Diplopterol is the major hopanoid in *M. extorquens* and is localized in the outer membrane (Hancock and Williams, 1986; Sáenz et al., 2015). We previously demonstrated that diplopterol has a sterol-like ability to modulate the order of saturated lipids such as lipopolysaccharides in the bacterial outer membrane (Sáenz et al., 2012). Subsequent work demonstrated that 2-methylation of hopanoids increases their membrane rigidifying effect (Sáenz et al., 2015; Wu et al., 2015). Therefore, variations in diplopterol 2-methylation could play a role in the adaptation of the outer membrane. While total diplopterol abundances (diplopterol + 2-methyl-diplopterol) did not vary substantially under any conditions, 2-methylation of diplopterol is highly variable in all conditions except methanol and detergent (Figure 7a and b). There is a progressive increase in 2-methyl-diplopterol abundance with decreasing temperature and increasing salt concentration (Figure 7c), consistent with transcriptional regulation of this process by global stress response pathways (Kulkarni et al., 2013). These results show for the first time that 2-methylation is dynamically regulated in response to varying growth conditions and is important for outer membrane adaptation.

Our observations highlight three characteristics of structural lipid adaptation. First, we observed that adaptivity of features over a particular range of conditions (e.g. temperature) does not involve a monotonic pattern of feature remodeling, but rather can involve different features over intervals of a given condition. Second, certain features such as acyl-chain unsaturation and diplopterol 2-methylation are highly variable and are remodeled over a broad range of conditions. However, other features such as lipid class and acyl-chain length are relatively invariant except under extreme conditions of low temperature and stationary growth stage, suggesting that chain length and

headgroup distribution have multiple constraints (e.g. maintaining membrane thickness or surface charge). Notably, even the tightly constrained features are adjusted under extreme perturbations. Third, acyl chain features are regulated independently within each headgroup class. Thus, even when total acyl-chain unsaturation and length appears invariant, there can be extensive acyl chain remodeling within specific headgroup classes. Such class-specific remodeling of unsaturation may result in adaptation that is localized to the inner or outer membrane, or to specific regions within each membrane, such as highly curved regions at the poles, one particular membrane leaflet, lipids that are closely associated with protein transmembrane domains, or potentially lateral membrane domains. On the other hand, constraining total unsaturation while internally shifting double bonds from PC to CL might be a means of varying intrinsic curvature while maintaining total membrane viscosity.

Summary and Outlook

In this study, we systematically characterized the lipidome of *M. extorquens* over a range of growth conditions to gain insights into membrane homeostatic adaptation. We demonstrated that membranes composed of only a few lipid species are capable of adapting specifically to a broad range of conditions, in particular temperature. Lastly, we showed that lipidomes must be assessed by lipid species composition, but also by the composite structural features conferred by binned combinations of lipids, such as the total number of double bonds or the global sum of acyl chain lengths, since combination of these structural features ultimately dictates the physical state and functionality of membranes.

We probed the lipidome composition across a broad range of viable conditions spanning temperature, hyperosmotic and detergent stress, carbon sources, and cell density. While individual lipid species do adapt to changing conditions, eight lipid species are variable in all experimental regimes (Figure 4) and the majority of lipids remained surprisingly stable. PCA analysis reveals that most lipidomes are highly similar across conditions (Figure 3). This demonstrates that the lipidome is robust and that there are strong constraints on lipidome composition and remodelling. One of the outstanding conundrums in membrane biology is to understand why there are so many lipids (Dowhan, 1997; 2017), even a relatively simple organism like *E. Coli* has over 100 phospholipid species (Jeucken et al., 2019). Recapitulating such a complex system from first principles seems daunting. However, the lipidome of *M. extorquens* demonstrates that a synthetic membrane capable of supporting life over a broad range of environmental conditions could be constructed with a relatively small number of lipid species.

306 The lipidome adaptability is also constrained by structural elements of individual lipids. Instead of
307 analysing lipidomes purely by lipid species, it is therefore critical to assess the global structural
308 composition. For example, total phospholipid chain length, that influences membrane thickness, is a
309 highly conserved feature that only varies under extreme conditions such as low temperature (Jensen
310 and Mouritsen, 2004). Interestingly, phospholipid acyl chain length was highly conserved globally,
311 but variable within certain headgroup classes. Other constraints do not have such clear implications.
312 For instance, phospholipid headgroup composition only varies at low temperature or in stationary
313 growth phase, possibly suggesting conservation of membrane surface charge as a key constraint.
314 Also, the acyl chain composition among phosophilpids with PG headgroup is nearly invariant across
315 all conditions, suggesting that there could be biochemical constraints on PG remodelling. Low PG
316 remodelling has also been observed in cyanobacteria (Pittera et al., 2018), showing that this constraint
317 is not limited to *M. extorquens*. In contrast, we learned that PC acyl chain composition is highly
318 variable and appears to take on the brunt of adaptive remodelling. While the physicochemical and
319 physiological basis for these observations remains to be fully explored, the patterns and constraints
320 in lipidome remodelling that we report here serve as a resource for designing a minimal adaptive
321 membrane and highlight the need for multi-level analysis of lipidome data.
322
323 Understanding how *M. extorquens* adapts with so few lipids, and even fewer that are responsive,
324 remains an open challenge. In particular, given that lipid remodelling did not involve a monotonic
325 change, but rather seemed to involve different features varying over different intervals of a given
326 range of conditions, such as temperature. One possibility is that the presence of isoprenoids, sterol-
327 like hopanoids, buffer changes in membrane properties and thereby minimizes the need for
328 phospholipid remodelling. Our previous data, however, shows that hopanoids primarily interact with
329 lipopolysaccharides in the outer leaflet of the outer membrane, and thus would not be relevant to
330 variations of the phospholipidome within the inner membrane or inner leaflet of the outer membrane
331 (Sáenz et al., 2015; 2012). Alternatively it has also been proposed that in bacterial membranes lacking
332 sterol analogues or complex lipidomes, integral membrane proteins may serve a role in adaptation
333 (Kaiser et al., 2011). Similarly unexplored are the sense and response pathways that underlie such
334 complex patterns of lipidome adaptation. It has emerged in recent years that there can be dedicated
335 membrane sensors, which are involved in regulating lipid biosynthesis pathways in response to
336 perturbed membrane properties (Ernst et al., 2016; Puth et al., 2015; Saita and de Mendoza, 2015). It
337 is presently unknown how many different sensors are required for adaptation, and how many
338 orthogonal parameters can be distinguished by such sensors. Building on the lipidomic resource
339 presented here, *M. extorquens* is a promising model organism to explore minimal mechanisms for

cell membrane adaptation. The adaptive lipidome of *M. extorquens* provides a critical resource as a starting point to elucidate the regulatory systems underlying membrane adaptation.

Acknowledgements

The authors wish to thank Kai Simons and Robert Ernst for advice, members of Sáenz group for discussions, Michael Schlierf, Ilya Levental, Alex Bradley, Carl Modes, and Christoph Zechner for manuscript comments, and the MPI-CBG Mass Spectrometry Facility.

Author contributions

Sandra Rizk and Daniel Grosser performed bacterial growth experiments. Andrej Schevchenko and Oksana Lavrynenko performed MS analysis. Grzegorz Chwastek contributed to writing, editing and data analysis. Michał Surma performed MS data analysis and editing. Magda Rucińska performed bioinformatics analysis. Helena Jambor conceived and designed the figures. James Sáenz conceived the project, obtained funding, supervised the project, and wrote the manuscript. All authors read, edited and approved the final manuscript.

Funding

This work was supported by the B CUBE of the TU Dresden, a Simons Foundation Fellowship (to JPS), a German Federal Ministry of Education and Research BMBF grant (to JPS, project # 03Z22EN12), and a VW Foundation “Life” grant (to JPS, project # 93089).

Methods

Media, growth conditions

For all cultivations a defined media, here referred to as Hypho-TMM, was used (Delaney et al., 2013). All liquid cultures were grown at 30°C and pH 7 with shaking at 150 rpm unless stated otherwise. For all experiments we used a strain of *M. extorquens PA1* with the cellulose synthase genes knocked out to minimize clumping and improve cell density measurements (Delaney et al., 2013). Cultures were started from a glycerol stock stored at -80°C were plated on Hypho-TMM agarose plate and grown at 30°C. A liquid pre-culture was set up by sterile picking a single colony and transferring it to 5 ml of Hypho-TMM. This pre-culture was grown over night to near stationary phase. The experimental culture was started by inoculation to OD_{600nm} 0,02 with pre-culture and grown until a final OD_{600nm} of 0,2 - 0,3 (early log-phase) was reached. Several conditions were tested including the influence of salinity, carbon source (MeOH vs. succinate), detergent (up to 5% Triton-X100) and temperature (6 – 30°C). Cells were also harvested at mid-, late- and stationary growth stages. A defined volume representing 6 OD units (1 OD unit = 1 mL of OD 1) was sampled and pelleted. The harvested cells were washed twice with fresh media. The pellet was snap frozen in liquid nitrogen and stored until further processing at -20°C.

Hypho-TMM recipe:

1,45 mM K_2HPO_4; 1,88 mM NaH_2PO_4; 45,6 µM sodium citrate; 1,2 µM $ZnSO_4$; 1 µM $MnCl_2$;
18 µM $FeSO_4$; 2 µM $(NH_4)_6Mo_7O_{24}$; 1 µM $CuSO_4$; 2 µM $CoCl_2$; Na_2WO_4; 0,5 mM $MgCl_2$;
8 mM $(NH_4)_2SO_4$; 20 µM $CaCl_2$
30 mM PIPES
15 mM succinate unless stated otherwise

Shotgun mass spectrometry

For the lipidomic analysis by mass spectrometry the lipids of our harvested cells were extracted twice by the method of Blight and Dyer (Bligh and Dyer, 1959). The total lipid extracts representing 6 OD units of *M. extorquens* were analyzed by quantitative shotgun lipidomics (Ejsing et al., 2009) adapted for the quantification of hopanoids (diplopterol, and 2-methyl-diplopterol). Absolute concentrations of diplopterol and methyl-diplopterol were determined using deuterated cholesterol as internal standard.

Measurement of phospholipids

In order to determine the phospholipid classes and species present in the bacterial extracts the MS/MS experiments were performed. Based on fragmentation of lipid species the total lipidome was represented by 4 phospholipid classes: phosphatidylcholine (PC), phosphatidylethanolamine (PE), phosphatidylglycerol (PG) and cardiolipin (CL). For absolute quantification extracts were diluted with MS mix containing the 0,5 μM PC (34:0), PE (34:0), PG (34:0) mixture and 0,05 μM CL (57:4). MS spectra were acquired on Q Exactive tandem mass spectrometer (Thermo Fisher Scientific, Bremen, Germany) equipped with a robotic nanoflow ion source TriVersa NanoMate (Advion BioSciences, Ithaca NY). Spectra were acquired in negative MS mode with the mass resolution of $R_{m/z\ 400}$ = 280000 with AGC target value of 10^6 and maximum injection time of 1 s in the range of masses 400 – 1000 m/z. Raw data were processed using LipidXplorer software (Herzog et al., 2012; 2011).

Measurement of diplopterol

The extract was dried down and re-dissolved in MS mix (7,5 mM ammonium acetate in isopropanol/methanol/chloroform 4:2:1) spiked with cholesterol D7 standard to the final concentration of 0,13 mM. MS spectra were acquired on Q Exactive tandem mass spectrometer (Thermo Fisher Scientific, Bremen, Germany) equipped with a robotic nanoflow ion source TriVersa NanoMate (Advion BioSciences, Ithaca NY). Gas backpressure was 1.25 psi and ionization voltage was 0.95 kV. Spectra were acquired in positive MS mode with the mass resolution of $R_{m/z\ 400}$ = 140000 with AGC target value of 10^6 and maximum injection time of 1 s in the range of masses 360 – 455 m/z. Raw data were processed using LipidXplorer software.

Data analysis

Lipid abundances (mol% of total) of biological triplicates for all conditions are provided in the supplementary materials. One of the replicates at 13 ˚C yielded erroneous abundance data due to a problem with the internal standard in that replicate and we have therefore excluded it from our analyses.

Variation of lipid species across experimental conditions was calculated by taking the standard deviation of lipid abundances for replicates over a given range of conditions (e.g. temperature, salt, etc.). Total lipidomic variation was calculated as the cumulative variation of individual lipid species for a given range of conditions.

Visualization of lipidome variation for all conditions was investigated with principle component analysis (PCA). PCA was performed by using the R prcomp function in RStudio with default parameters, where the calculation is carried out by a singular value decomposition of the (centered and scaled) data matrix. Visualization in single plots performed using the ggbiplot function. PCA allows the identification of latent variables (principal components) in the data based on 14 observed variables. The plot is based on principal components 1 and 2, which explain 50.1% and 16.5% of the total variance of the data, respectively.

Variations in abundance of lipid features were analyzed by binning lipid species according to structural features including total chain length, saturation, class (e.g. phospholipid head group and diplopterols), and 2-methylation of diplopterol. Acyl chain length and saturation were binned for all phospholipids (global acyl chain features), and separately within each head group (head group specific acyl chain features).

Figure Captions

Figure 1. Overview of experimental outline and lipids analyzed in this study. (A) Overview of experimental design and exemplary data obtained. **(B)** Schematic of lipid structural features measured in this study: headgroups of phospholipids and isoprenoids, acyl chain length and acyl chain saturation (number of double bonds).

Figure 1-figure supplement 1. Bacterial growth rates (Herbert et al., 1956) for all experimental conditions.

Figure 2. Table of lipid species abundances. Lipid species are annotated by class/headgroup (PG, PE, PC, CL or diplopterol), total acyl chain length (32 to 72), and total acyl chain saturation (number of double bonds per lipid, 0 to 4). Abundance is shown as percentage of total lipids per experiment. The range in abundance across all experimental conditions is indicated by individual grey dots, the abundances for the standard growth condition (30 ˚C, early exponential stage, 0.15 M sucrose) are shown in red.

Figure 3. Effect of experimental conditions on lipidomic variability. (A) Total lipidomic variability is given as the cumulative standard deviation of individual lipid species across each set of experimental conditions. Lipid variability is highest when varying temperature, and lowest in increasing percentage of detergent. **(B)** Principle component analysis (PCA) of the lipid species abundances shows the degree of variation between subconditions. The standard growth condition (30 ˚C, early exponential stage, 0.15 M sucrose) is indicated in red, and all other subconditions are grey. Again, lipidomes vary greatly in changing temperatures regimes, and also when bacteria enter stationary phase growth.

Figure 4. Variability of individual lipid species across experimental conditions. (A) Average abundances of lipid species for all conditions sorted from highest (PG 36:2) to lowest (CL 64:0) lipid species. Mean and range are shown for each lipid. **(B)** Heat map of lipid species variability across experimental conditions, high variability is indicated in red, no variability in light yellow. **(B')** Exemplary calculation of standard deviation. **(C)** UpSetR plot (Conway et al., 2017) showing the overlap of lipids adapting their amounts across the experimental conditions. Eight lipids vary their abundance in all experimental conditions, four lipids vary abundance specifically in changing temperatures. Stage: bacterial growth stage/phase, TX: varying detergent concentrations.

Figure 5. Variability of phospholipid structural features across experimental conditions. (A) Abundances of lipids grouped by lipid class shows overall low variability, and lowest variability of CL. **(B)** Abundances of phospholipid headgroup binned by acyl chain length and acyl chain saturation respectively reveals group specific differences in acyl chain remodelling. (headgroups blue = PG, green = PE, olive = PC, magenta = CL). **(A), (B)** each data point shows lipid abundance from individual biological replicates. **(C)** Variability of lipid features plotted for each set of experimental conditions. Stage: bacterial growth stage/phase, TX: varying detergent concentrations.

Figure 6. Step-wise adaptation of lipids by feature at changing environmental growth conditions. (A) Abundances of lipids grouped by class, acyl chain length and acyl chain saturation when changing growth temperature, probing at different growth stages, and varying salt (NaCl) concentration of the growth media. **(B)** Abundances of phospholipids grouped by acyl chain features, with headgroups indicated by color (blue: PG, green: PE, olive: PC, magenta: CL). This reveals compensatory effects in lipid adaptability: while abundance of PC with 2 double bonds increases with

494 increasing temperatures, PC with 3 double bonds decreases from 6 to 30 degrees. In each panel, the
495 most variable features are highlighted in bold.
496
497 **Figure 7. Diplopterol (hopanoid) methylation (A)** Abundances of diplopterol species across growth
498 conditions. **(B)** Step-wise adaptation of diplopterols whne changing temperature, grpwth phase, and
499 salt condition.
500
501 **Figure 1 – Supplement 1** Graphical abstract
502 **Figure 1 – Supplement 2** Bacterial growth curves and sampling points for lipidomic analysis. Chart
503 for growth phases is a conceptual drawing.
504 **Figure 6 - Supplement 1** Overview of compositional changes across exemplary experimental
505 conditions reveals the lipidome is robust in most growth conditions except in drastic temperature
506 changes when the lipidome is markedly different.
507 **Figure 6 - Supplement 2.** Step-wise adaptation of lipids by feature sampled at varying growth
508 temperatures.
509 **Figure 6 - Supplement 3.** Step-wise adaptation of lipids by feature sampled at early, late, mid and
510 stationary growth phase.
511 **Figure 6 - Supplement 4.** Step-wise adaptation of lipids by feature sampled at varying salt
512 concentrations (NaCl).
513
514
515
516
517
518
519
520
521

References

Bligh, E.G., and Dyer, W.J. (1959). A Rapid Method of Total Lipid Extraction and Purification. Canadian Journal of Biochemistry and Physiology *37*, 911–917.

Bradley, A.S., Swanson, P.K., Muller, E.E.L., Bringel, F., Caroll, S.M., Pearson, A., Vuilleumier, S., and Marx, C.J. (2017). Hopanoid-free Methylobacterium extorquens DM4 overproduces carotenoids and has widespread growth impairment. PLoS ONE *12*, e0173323.

Conway, J.R., Lex, A., and Gehlenborg, N. (2017). UpSetR: an R package for the visualization of intersecting sets and their properties. Bioinformatics *33*, 2938–2940.

Delaney, N.F., Kaczmarek, M.E., Ward, L.M., Swanson, P.K., Lee, M.C., and Marx, C.J. (2013). Development of an optimized medium, strain and high-throughput culturing methods for Methylobacterium extorquens. PLoS ONE *8*, e62957.

Dowhan, W. (1997). Molecular basis for membrane phospholipid diversity: why are there so many lipids? Annu Rev Biochem.

Dowhan, W. (2017). Understanding phospholipid function: Why are there so many lipids? J. Biol. Chem. *292*, 10755–10766.

Ejsing, C.S., Sampaio, J.L., Surendranath, V., Duchoslav, E., Ekroos, K., Klemm, R.W., Simons, K., and Shevchenko, A. (2009). Global analysis of the yeast lipidome by quantitative shotgun mass spectrometry. Proceedings of the National Academy of Sciences *106*, 2136–2141.

Ernst, R., Ejsing, C.S., and Antonny, B. (2016). Homeoviscous Adaptation and the Regulation of Membrane Lipids. Journal of Molecular Biology *428*, 4776–4791.

Gorter, E., and Grendel, F. (1925). On biomolecular layers of lipoids on the chromocytes of the blood. J Exp Med *41*, 439–443.

Hancock, I., and Williams, K. (1986). The outer membrane of Methylobacterium organophilum. Microbiology.

Hardy, M.D., Yang, J., Selimkhanov, J., Cole, C.M., Tsimring, L.S., and Devaraj, N.K. (2015). Self-reproducing catalyst drives repeated phospholipid synthesis and membrane growth. P Natl Acad Sci Usa *112*, 8187–8192.

Helenius, A. (1975). Solubilization of membranes by detergents. Biochim Biophys Acta.

Herzog, R., Schuhmann, K., Schwudke, D., Sampaio, J.L., Bornstein, S.R., Schroeder, M., and Shevchenko, A. (2012). LipidXplorer: A Software for Consensual Cross-Platform Lipidomics. PLoS ONE *7*, e29851.

Herzog, R., Schwudke, D., Schuhmann, K., Sampaio, J.L., Bornstein, S.R., Schroeder, M., and Shevchenko, A. (2011). A novel informatics concept for high-throughput shotgun lipidomics based on the molecular fragmentation query language. Genome Biol. *12*, R8.

Hunte, C., and Richers, S. (2008). Lipids and membrane protein structures. Curr Opin Struct Biol *18*, 406–411.

559 Jensen, M., and Mouritsen, O. (2004). Lipids do influence protein function - the hydrophobic
560 matching hypothesis revisited. BBA-Biomembranes *1666*, 205–226.

561 Jeucken, A., Molenaar, M.R., van de Lest, C.H.A., Jansen, J.W.A., Helms, J.B., and Brouwers, J.F.
562 (2019). A Comprehensive Functional Characterization of Escherichia coli Lipid Genes. Cell Rep
563 *27*, 1597–1606.e2.

564 Kaiser, H.-J., Surma, M.A., Mayer, F., Levental, I., Grzybek, M., Klemm, R.W., Da Cruz, S.,
565 Meisinger, C., Müller, V., Simons, K., et al. (2011). Molecular Convergence of Bacterial and
566 Eukaryotic Surface Order. J Biol Chem *286*, 40631–40637.

567 Klose, C., Surma, M.A., and Simons, K. (2013). Organellar lipidomics-background and
568 perspectives. Curr Opin Cell Biol.

569 Klose, C., Surma, M.A., Gerl, M.J., Meyenhofer, F., Shevchenko, A., and Simons, K. (2012).
570 Flexibility of a Eukaryotic Lipidome – Insights from Yeast Lipidomics. PLoS ONE *7*, e35063.

571 Kulkarni, G., Wu, C.-H., and Newman, D.K. (2013). The General Stress Response Factor EcfG
572 Regulates Expression of the C-2 Hopanoid Methylase HpnP in *Rhodopseudomonas palustris* TIE-1.
573 J Bacteriol *195*, 2490–2498.

574 Nikaido, H. (1996). Multidrug efflux pumps of gram-negative bacteria. J Bacteriol *178*, 5853–5859.

575 Nikaido, H. (2003). Molecular basis of bacterial outer membrane permeability revisited.
576 Microbiology and Molecular Biology Reviews *67*, 593–656.

577 Nikaido, H., and Vaara, M. (1985). Molecular-Basis of Bacterial Outer-Membrane Permeability.
578 Microbiol Rev *49*, 1–32.

579 Piddock, L.J.V. (2006). Multidrug-resistance efflux pumps - not just for resistance. Nat Rev Micro
580 *4*, 629–636.

581 Pittera, J., Jouhet, J., Breton, S., Garczarek, L., Partensky, F., Maréchal, É., Nguyen, N.A., Doré,
582 H., Ratin, M., Pitt, F.D., et al. (2018). Thermoacclimation and genome adaptation of the membrane
583 lipidome in marine Synechococcus. Environ Microbiol *20*, 612–631.

584 Pomorski, T., and Menon, A.K. (2006). Lipid flippases and their biological functions. Cell Mol Life
585 Sci *63*, 2908–2921.

586 Puth, K., Hofbauer, H.F., Sáenz, J.P., and Ernst, R. (2015). Homeostatic control of biological
587 membranes by dedicated lipid and membrane packing sensors. Biol Chem *396*, 1043–1058.

588 Rashby, S.E., Sessions, A.L., Summons, R.E., and Newman, D.K. (2007). Biosynthesis of 2-
589 methylbacteriohopanepolyols by an anoxygenic phototroph. Proceedings of the National Academy
590 of Sciences *104*, 15099–15104.

591 Ricci, J.N., Coleman, M.L., Welander, P.V., Sessions, A.L., Summons, R.E., Spear, J.R., and
592 Newman, D.K. (2014). Diverse capacity for 2-methylhopanoid production correlates with a specific
593 ecological niche. The ISME Journal *8*, 675–684.

594 Saita, E.A., and de Mendoza, D. (2015). Thermosensing via transmembrane protein–lipid
595 interactions. Biochimica Et Biophysica Acta (BBA)-Biomembranes *1848*, 1757–1764.

596 Sanders, C.R., and Mittendorf, K.F. (2011). Tolerance to Changes in Membrane Lipid Composition
597 as a Selected Trait of Membrane Proteins. Biochemistry *50*, 7858–7867.

598 Sáenz, J.P., Grosser, D., Bradley, A.S., Lagny, T.J., Lavrynenko, O., Broda, M., and Simons, K.
599 (2015). Hopanoids as functional analogues of cholesterol in bacterial membranes. P Natl Acad Sci
600 Usa *112*, 11971–11976.

601 Sáenz, J.P., Sezgin, E., Schwille, P., and Simons, K. (2012). Functional convergence of hopanoids
602 and sterols in membrane ordering. Proceedings of the National Academy of Sciences *109*, 14236–
603 14240.

604 Singer, S.J., and Nicolson, G.L. (1972). The fluid mosaic model of the structure of cell membranes.
605 Science *175*, 720–731.

606 Stampf, P., Herrmann, D., Bisseret, P., and Rohmer, M. (1991). 2α-Methylhopanoids: First
607 Recognition in the Bacterium Methylobacterium organophilum and Obtention via Sulphur Induced
608 Isomerization of 2ß-Methylhopanoids. Tetrahedron *47*, 7081–7090.

609 Summons, R.E., Jahnke, L.L., Hope, J.M., and Logan, G.A. (1999). 2-Methylhopanoids as
610 biomarkers for cyanobacterial oxygenic photosynthesis. Nature *400*, 554–557.

611 van Meer, G., Voelker, D.R., and Feigenson, G.W. (2008). Membrane lipids: where they are and
612 how they behave. Nat Rev Mol Cell Bio *9*, 112–124.

613 Wallace, P., Hollis, D., and Weaver, R. (1990). Biochemical and chemical characterization of pink-
614 pigmented oxidative bacteria. Journal of Clinical ….

615 Wu, C.-H., Bialecka-Fornal, M., and Newman, D.K. (2015). Methylation at the C-2 position of
616 hopanoids increases rigidity in native bacterial membranes. eLife *4*.

617

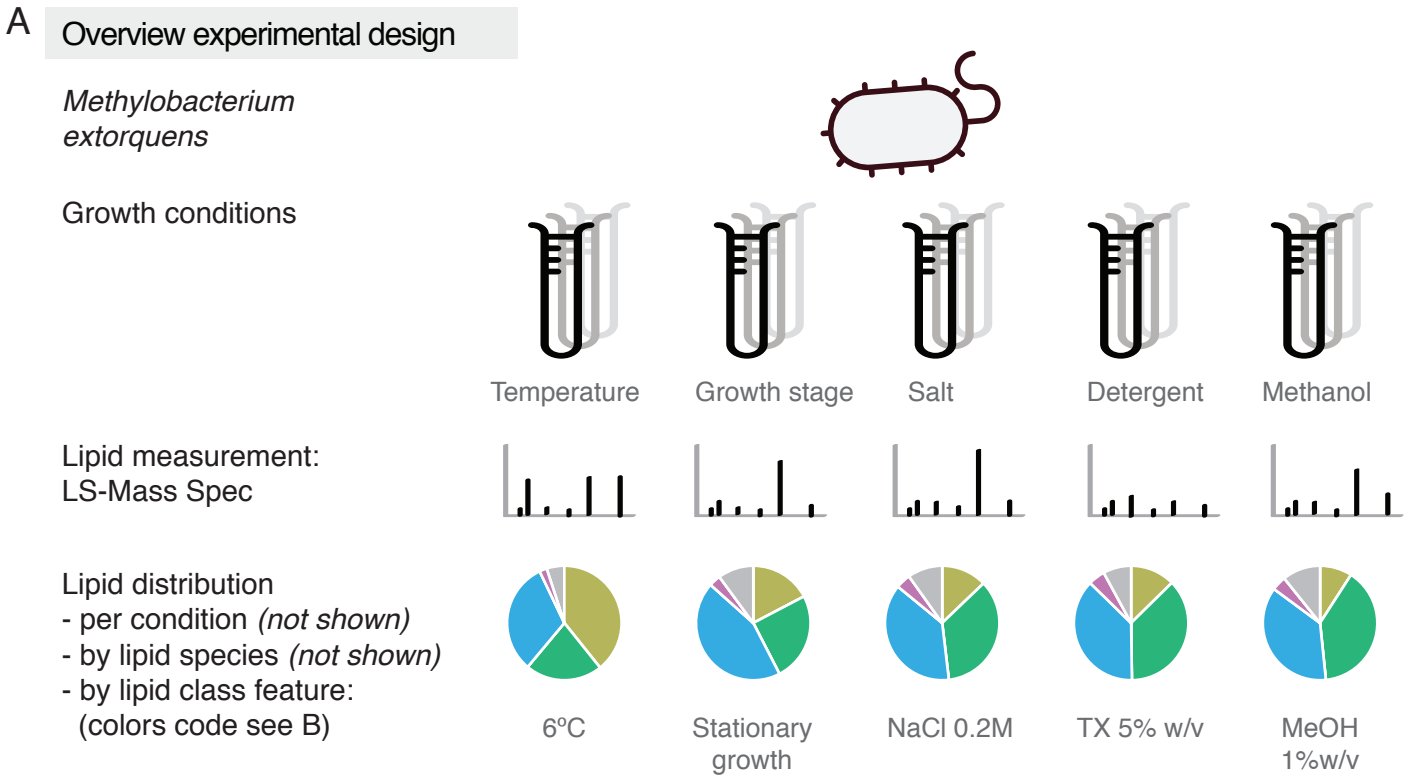

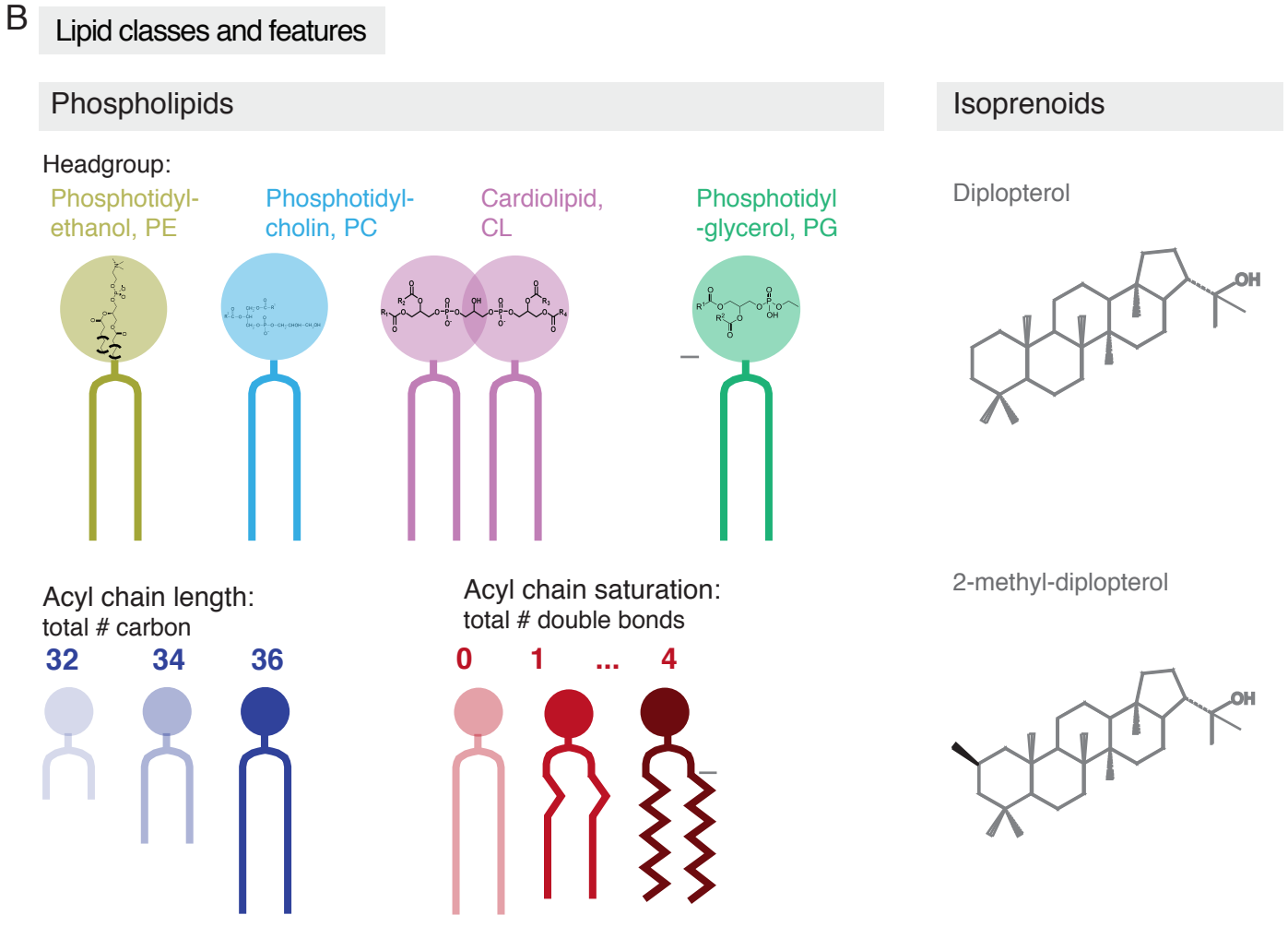

Figure 1. Overview of experimental outline and lipids analysed in this study. (A) Overview of experimental design and exemplary data obtained. **(B)** Schematic of lipid structural features measured in this study: head groups of phosopholipids and isoprenoids, acyl chain length and acyl chain saturation (number of double bonds).

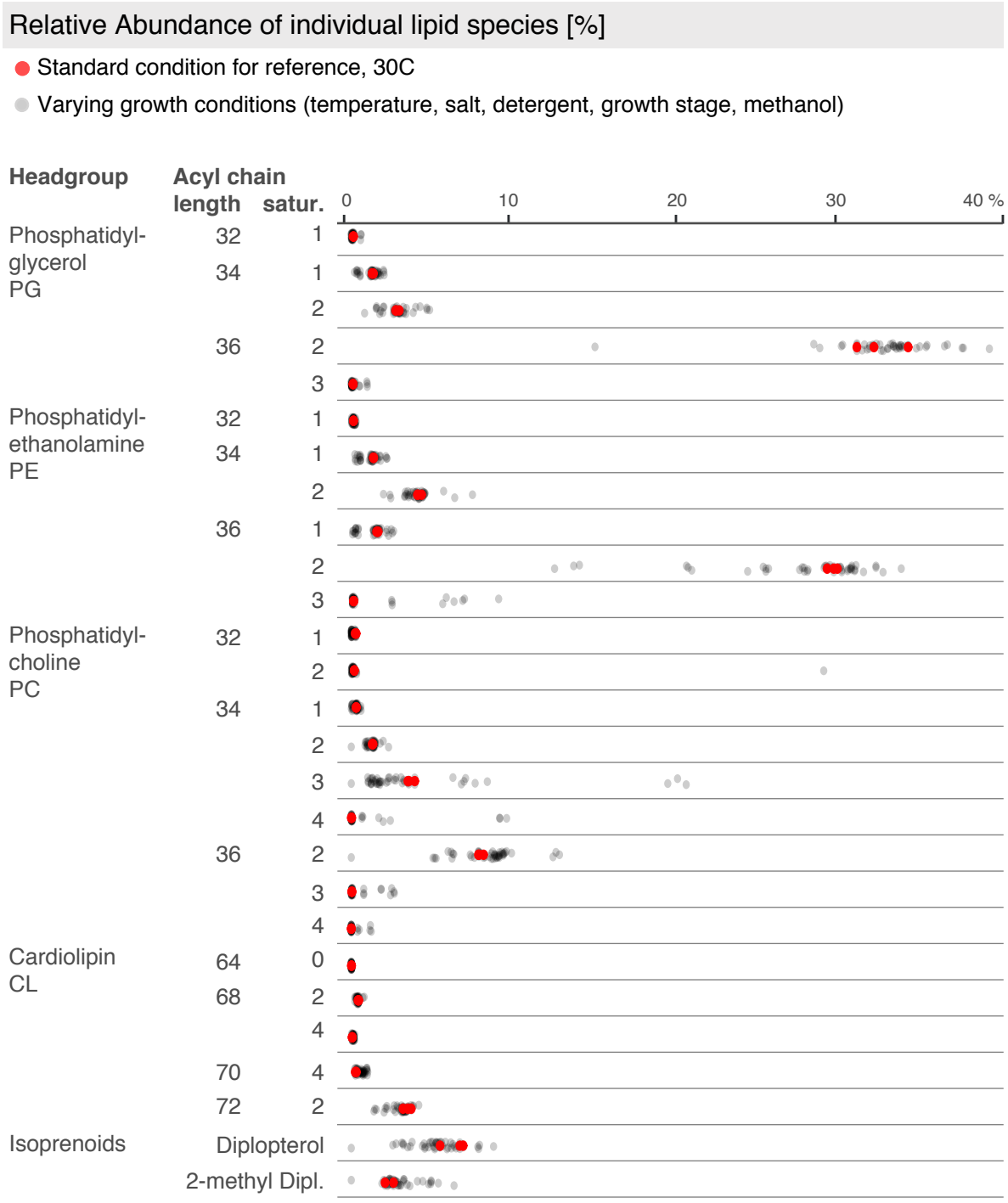

Figure 2. Table of lipid species abundances. Lipid species are annotated by class/head group (PG, PE, PC, CL or diplopterol), total acyl chain length (32 to 72), and total acyl chain saturation (number of double bonds per lipid, 0 to 4). Abundance is shown as percentage of total lipids per experiment. The range in abundance across all experimental conditions is indicated by individual grey dots, the abundances for the standard growth condition (30 ˚C, early exponential stage, 0.15 M sucrose) are shown in red.

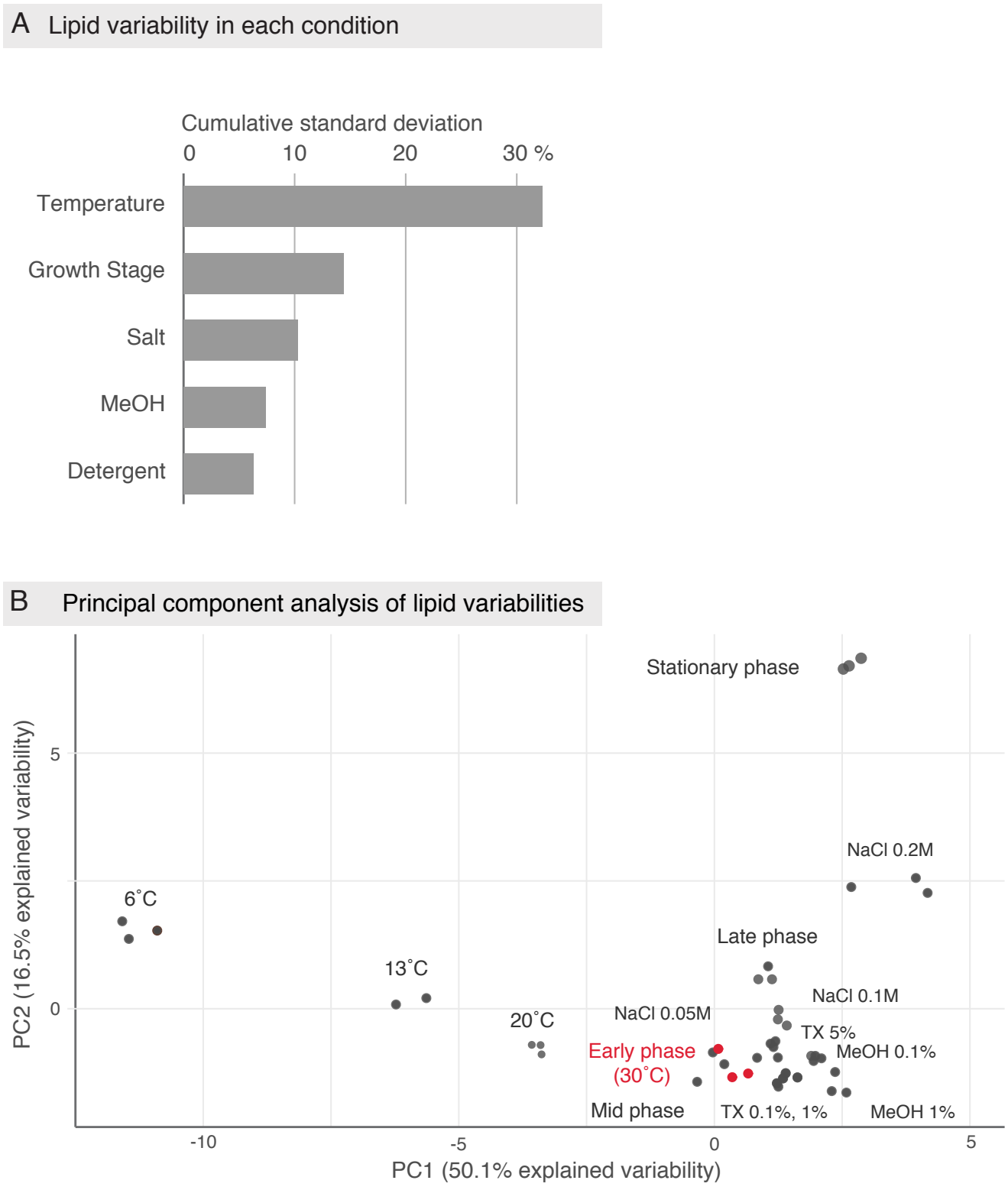

Figure 3. Effect of experimental conditions on lipidomic variability. (A) Total lipidomic variability is given as the cumulative standard deviation of individual lipid species across each set of experimental conditions. Lipid variability is highest when varying temperature, and lowest in increasing percentage of detergent. **(B)** Principle component analysis (PCA) of the lipid species abundances shows the degree of variation between subconditions. The standard growth condition (30 ˚C, early exponential stage, 0.15 M sucrose) is indicated in red, and all other subconditions are grey. Again, lipidomes vary greatly in changing temperatures regimes, and also when bacteria enter stationary phase growth. TX = detergent

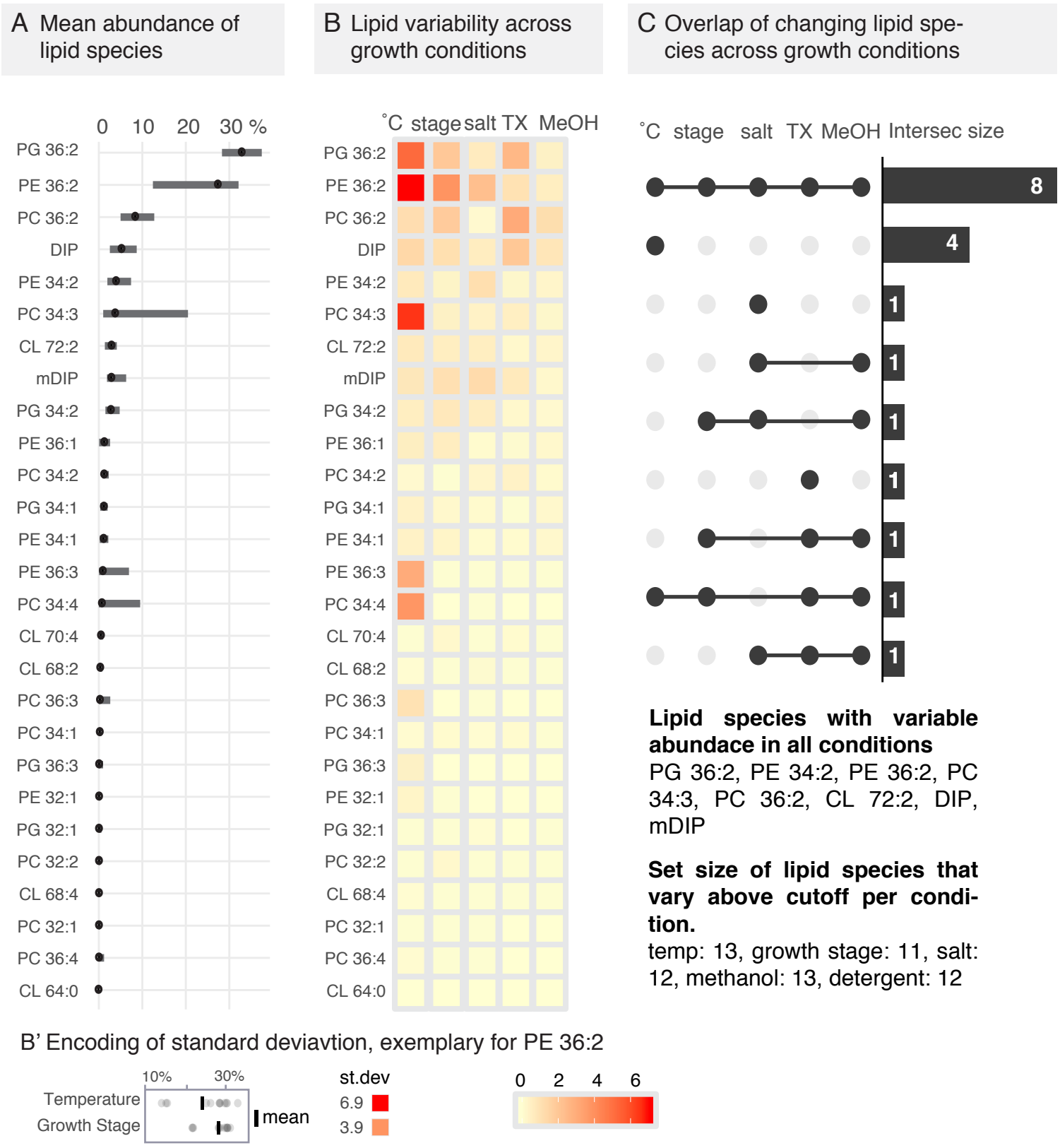

Figure 4. Variability of individual lipid species across experimental conditions. (A) Average abundances of lipid species for all conditions sorted from highest (PG 36:2) to lowest (CL 64:0) lipid species. Mean and range are shown for each lipid. **(B)** Heat map of lipid species variability across experimental conditions, high variability is indicated in red, no variability in light yellow. (B') Exemplary calculation of standard deviation. **(C)** UpSetR plot (Conway, 2017) showing the overlap of lipids adapting their amounts across the experimental conditions. Eight lipids vary their abundance in all experimental conditions, four lipids vary abundance specifically in changing temperatures. stage = growth stage/phase, TX = varying detergent concentrations.

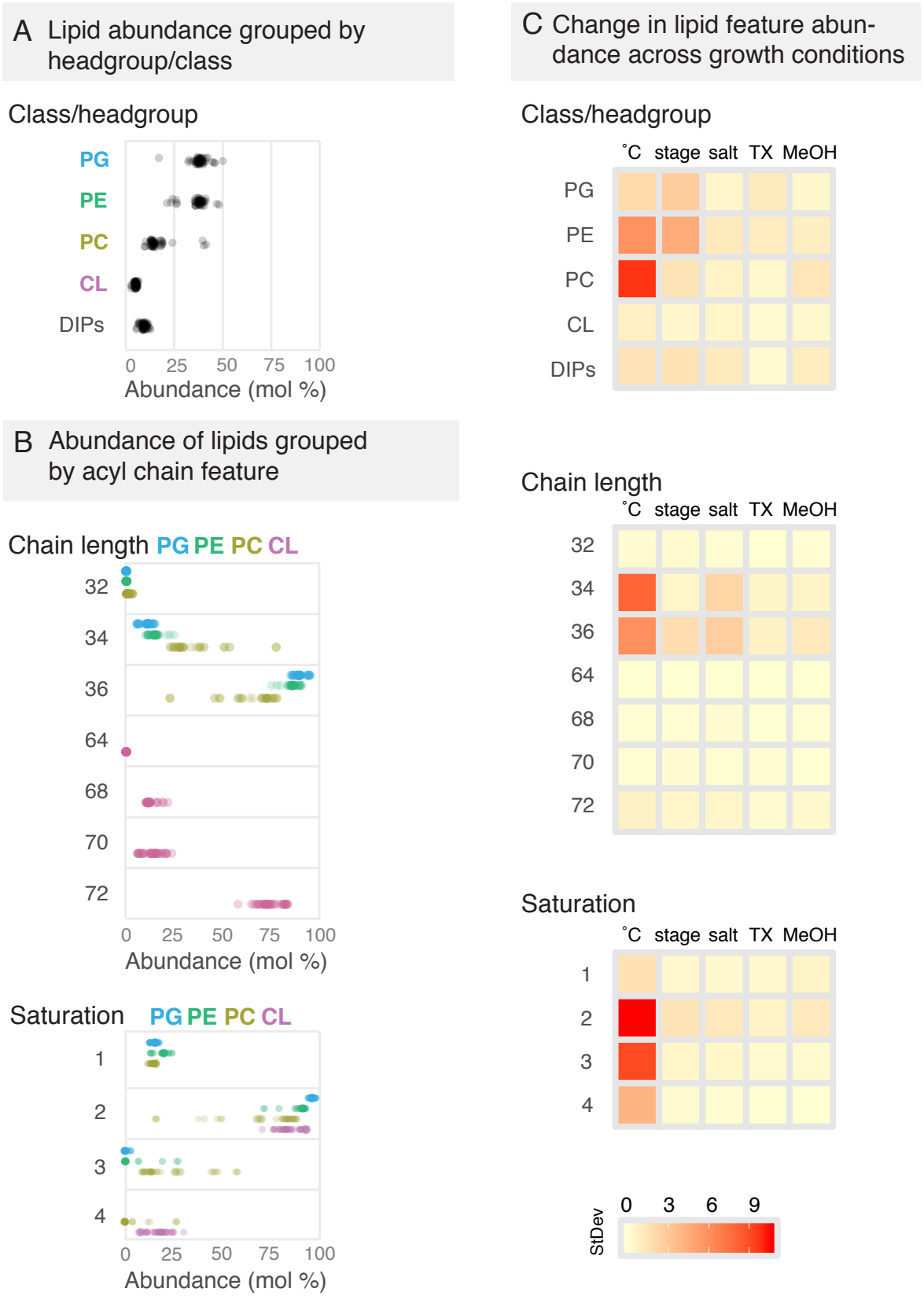

Figure 5. Variability of phospholipid structural features across experimental conditions. **(A)** Abundances of lipids grouped by lipid class shows overall low variability, and lowest variability of CL. **(B)** Abundances of phospholipid headgroup binned by acyl chain length and acyl chain saturation respectively reveals group specific differences in acyl chain remodelling. (headgroups blue = PG, green = PE, olive = PC, magenta = CL). **(A), (B)** each data point shows mean lipid amount from three biological replicates. **(C)** Variability of lipid features plotted for each set of experimental conditions. Stage: bacterial growth stage/phase, TX: varying detergent concentrations.

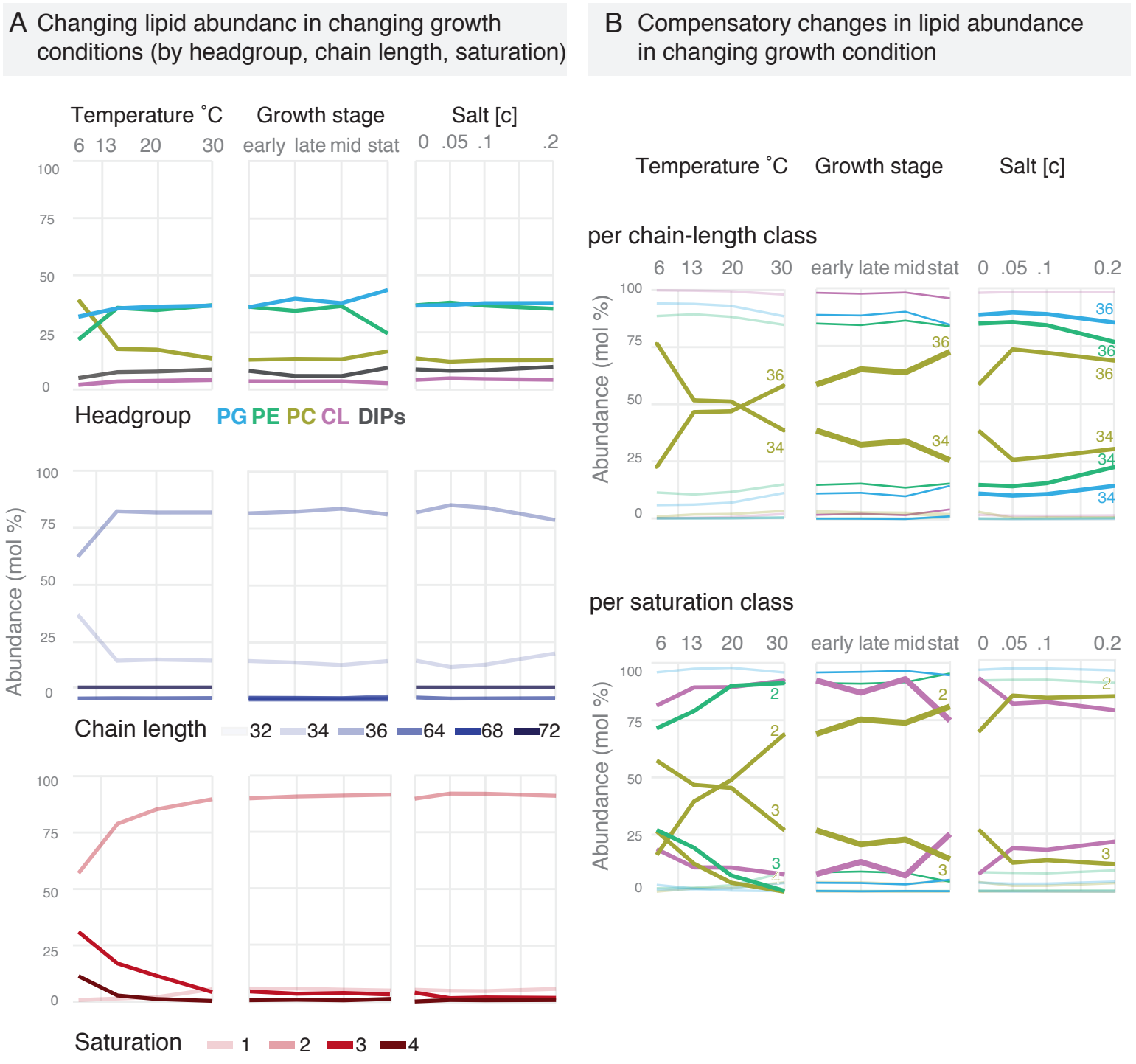

Figure 6. Step-wise adaptation of lipids by feature at changing environmental growth conditions. (A) Abundances of lipids grouped by class, acyl chain length and acyl chain saturation when changing growth temperature, probing at different growth stages, and varying salt (NaCl) concentration of the growth media. **(B)** Abundances of phospholipids grouped by acyl chain features, with headgroups indicated by color (blue: PG, green: PE, olive: PC, magenta: CL). This reveals compensatory effects in lipid adaptability: while abundance of PC with 2 double bonds increases with increasing temperatures, PC with 3 double bonds decreases from 6 to 30 degrees. In each panel, the most variable features are highlighted in bold.

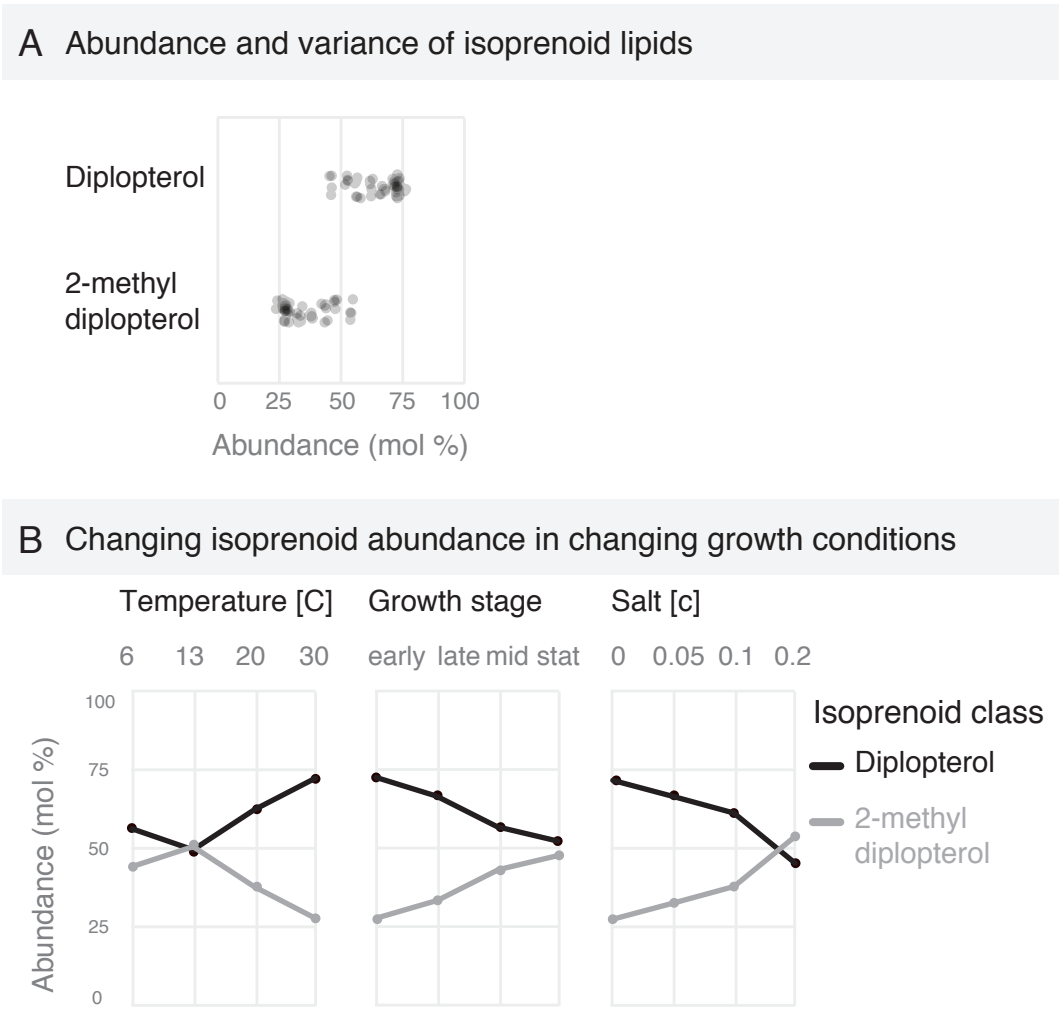

Figure 7. Diplopterol (hopanoid) methylation (A) Abundances of diplopterol species across growth conditions. **(B)** Step-wise adaptation of diplopterols when changing temperature, growth phase, and salt condition.

Methylobacterium extorquens
Gram-negative plant-based model to explore membrane adaptability

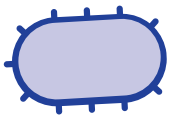

Systematic exploration of diverse enviornmental conditions
The standard growth condition (30°C, early phase) was adapted to new regimes.

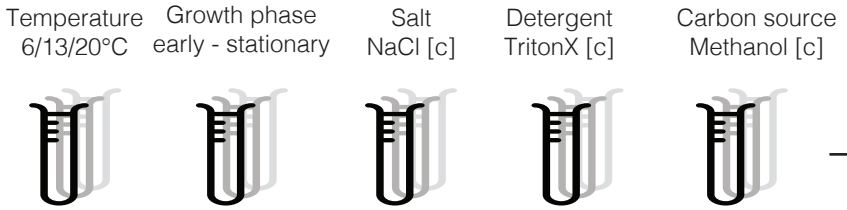

Quantitative Mass-spec
Lipids were quantitatively measured by LS-Mass Spec

PCA showes robust lipidome across conditions, remodeling is notable in variable temperature con-

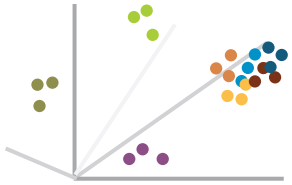

Variability across conditions: 8 lipid species were adapted in all conditions.

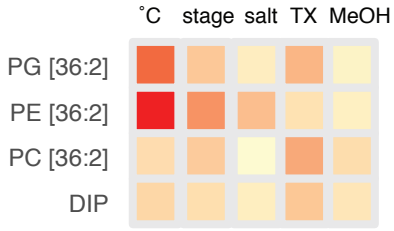

Lipidome composition by lipid feature remodelling e.g. of headgroup/class shows robustness also at the lipid structure level.

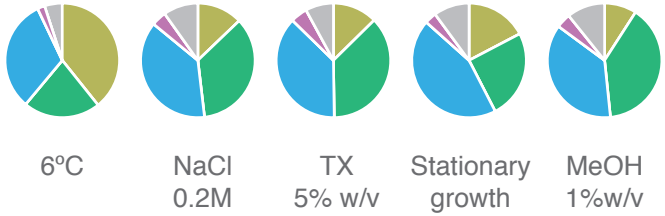

Figure 1 - supplement 1 Graphical abstract

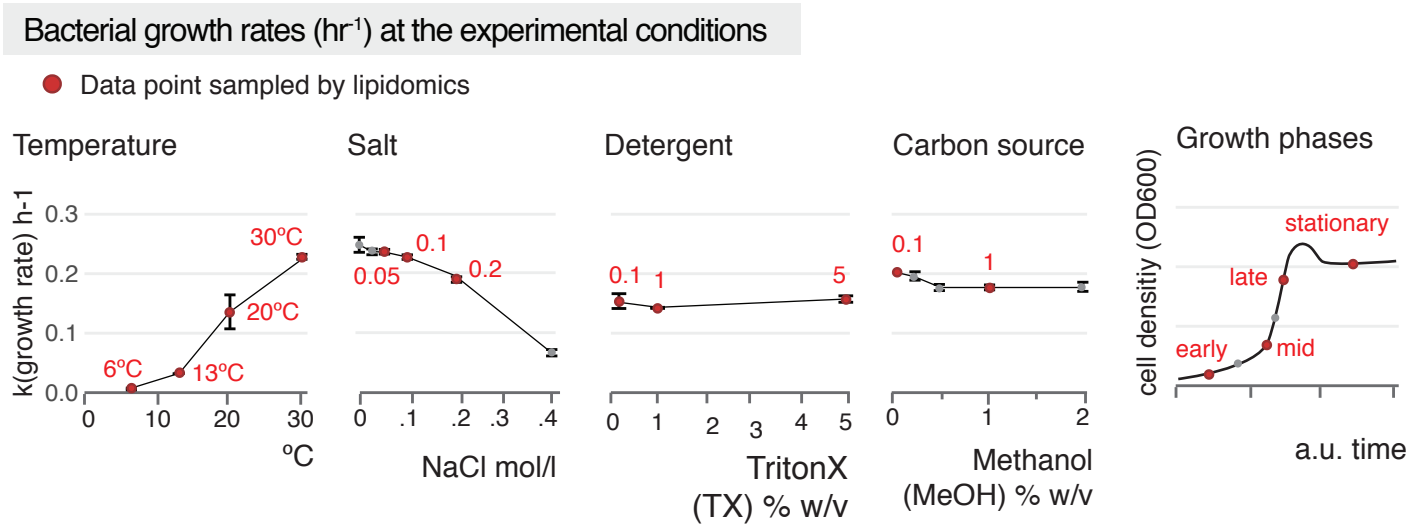

Figure 1 – Supplement 2 Bacterial growth curves and sampling points for lipidomic analysis. Chart for growth phases is a conceptual drawing.

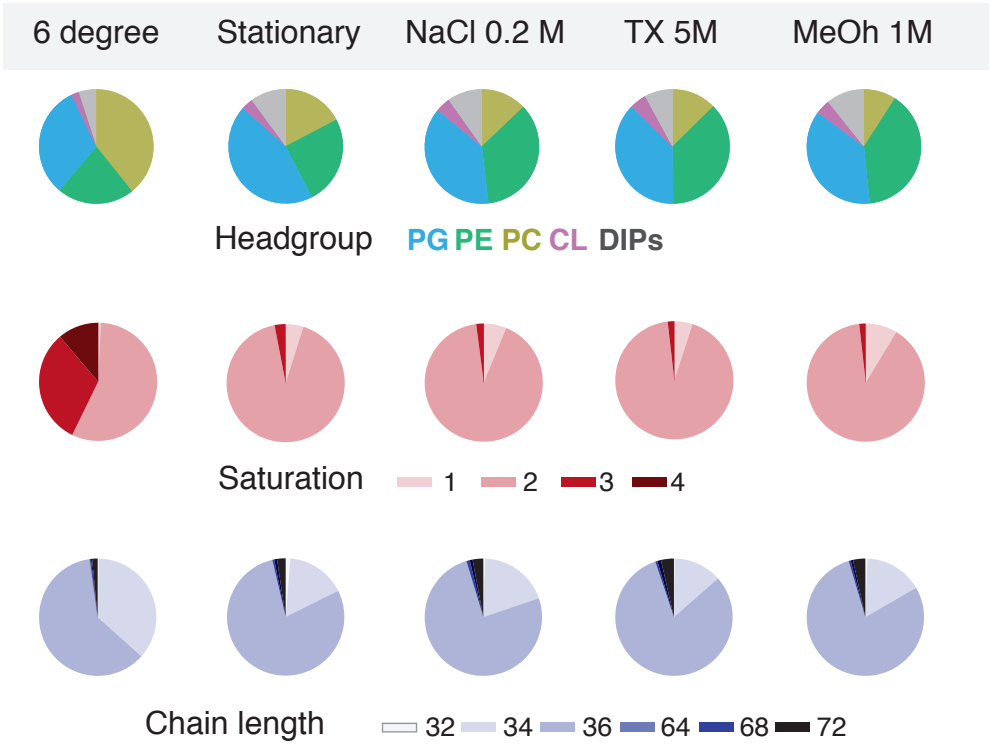

Figure 6 - Supplement 1 Overview of compositional changes across exemplary experimental conditions reveals the lipidome is robust in most growth conditions except in drastic temperature changes when the lipidome is markedly different.

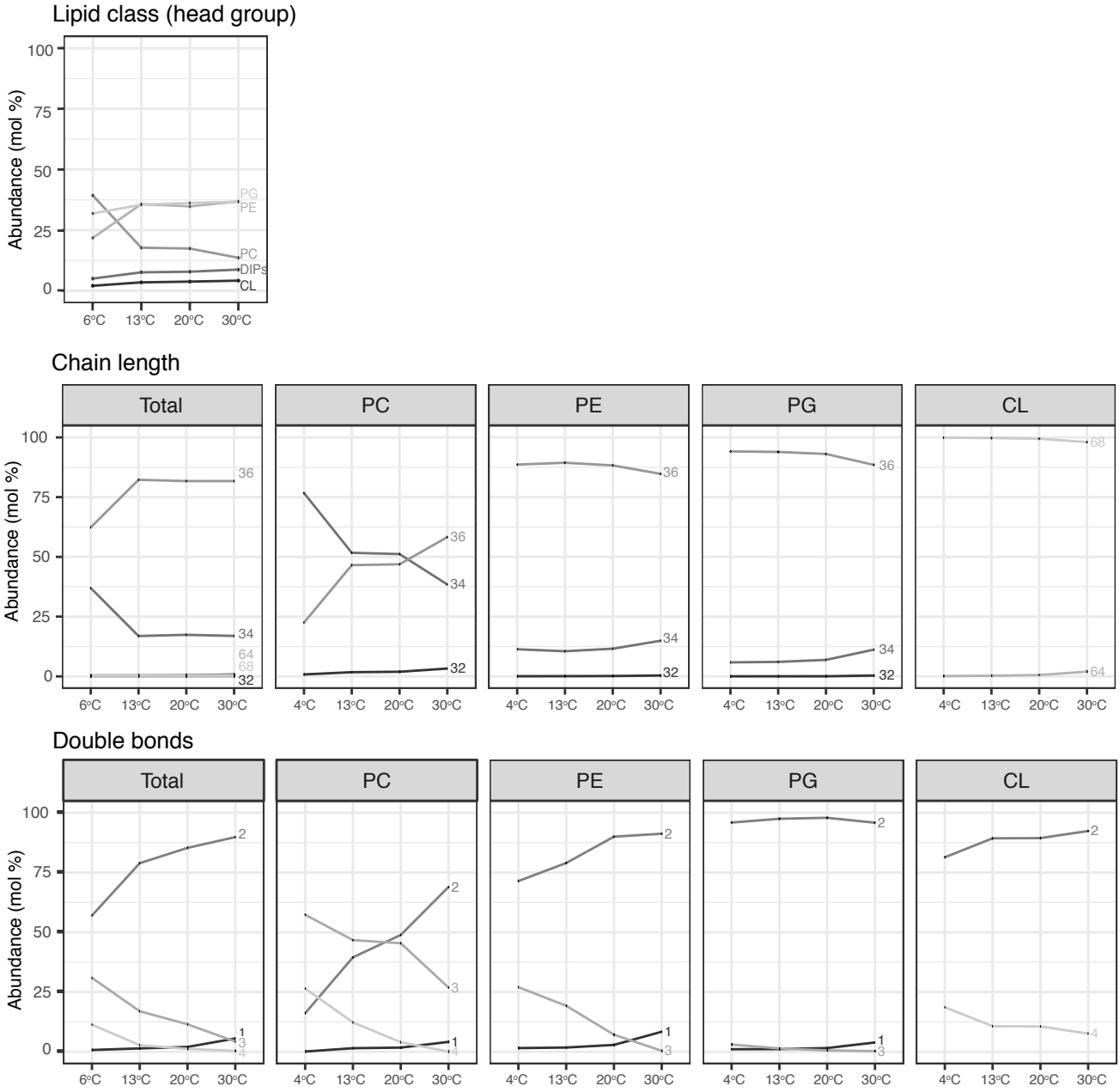

Figure 6 - Supplement 2. Step-wise adaptation of lipids by feature sampled at varying growth temperatures.

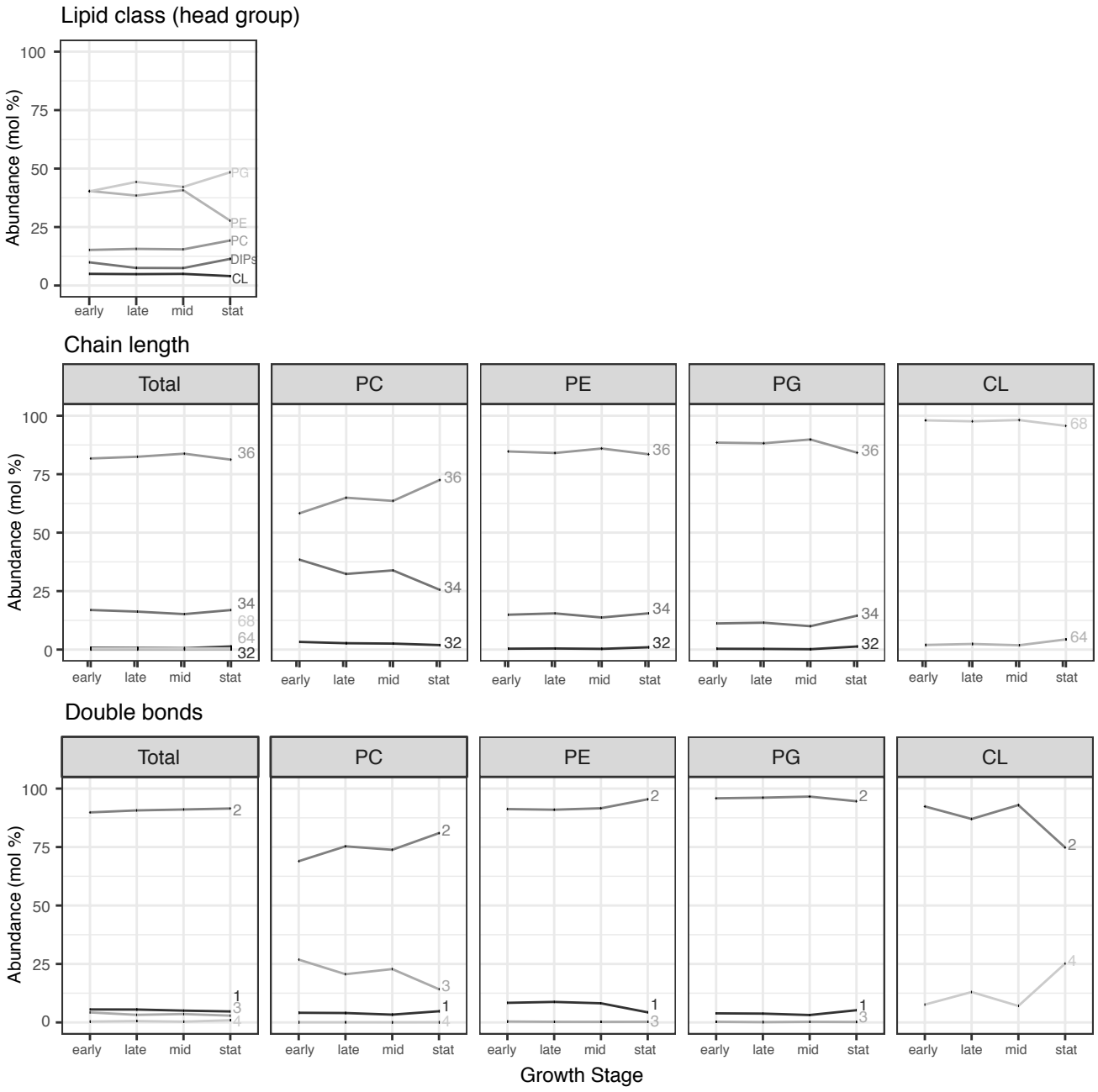

Figure 6 - Supplement 3. Step-wise adaptation of lipids by feature sampled at early, late, mid and stationary growth phase.

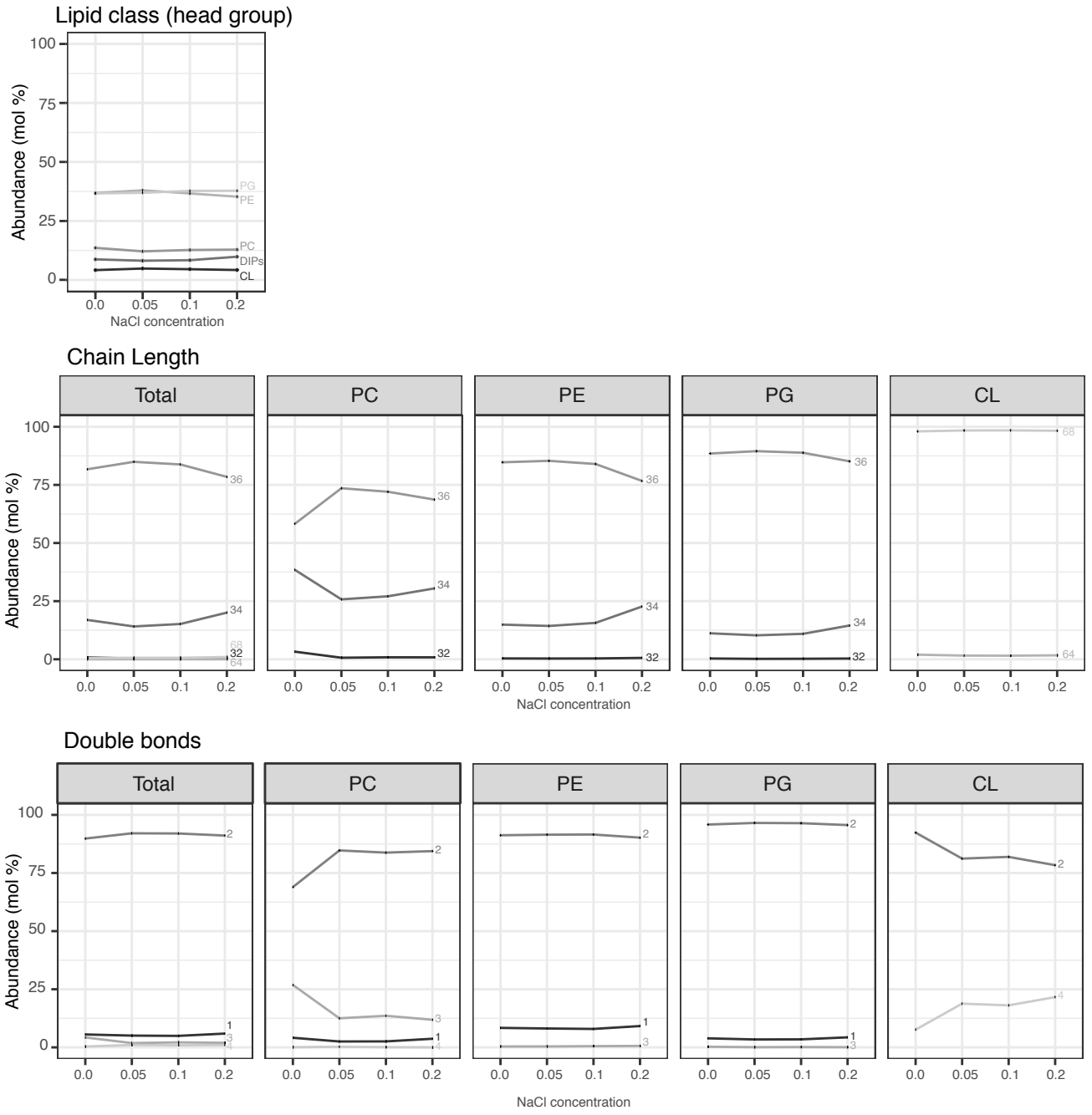

Figure 6 - Supplement 4. Step-wise adaptation of lipids by feature sampled at varying salt concentrations (NaCl).